

GALEX UV OBSERVATIONS OF THE INTERACTING GALAXY NGC 4438 IN THE VIRGO CLUSTER.

A. BOSELLI¹, S. BOISSIER², L. CORTESE¹, A. GIL DE PAZ², V. BUAT¹, J. IGLESIAS-PARAMO¹, B. F. MADORE^{2,8}, T. BARLOW³, L. BIANCHI⁴, Y.-I. BYUN⁵, J. DONAS¹, K. FORSTER³, P. G. FRIEDMAN³, T. M. HECKMAN⁶, P. JELINSKY⁷, Y.-W. LEE⁵, R. MALINA¹, D. C. MARTIN³, B. MILLIARD¹, P. MORRISSEY³, S. NEFF⁹, R. M. RICH¹⁰, D. SCHIMINOVICH³, M. SEIBERT³, O. SIEGMUND⁷, T. SMALL³, A. S. SZALAY⁶, B. WELSH⁷, T. K. WYDER³

Draft version June 29, 2018

ABSTRACT

We present GALEX NUV (2310Å) and FUV (1530Å) images of the interacting galaxy NGC 4438 (Arp 120) in the center of the Virgo cluster. These images show an extended (20 kpc) tidal tail at the north-west edge of the galaxy previously undetected at other wavelengths, at 15-25 kpc from its nucleus. Except in the nucleus, the UV morphology of NGC 4438 is totally different from the H α + [NII] one, more similar to the X-ray emission, confirming its gas cooling origin. We study the star formation history of NGC 4438 combining spectro-photometric data in the UV-visible-near-IR wavelength range with population synthesis and galaxy evolution models. The data are consistent with a recent (~ 10 Myr), instantaneous burst of star formation in the newly discovered UV north-western tail which is significantly younger than the age of the tidal interaction with NGC 4435, dated by dynamical models at ~ 100 Myr ago. Recent star formation events are also present at the edge of the northern arm and in the southern tail, while totally lacking in the other regions, which are dominated by the old stellar population perturbed during the dynamical interaction with NGC 4435. The contribution of this recent starburst to the total galaxy stellar mass is lower than 0.1%, an extremely low value for such a violent interaction. High-velocity, off-center tidal encounters such as that observed in Arp 120 are thus not sufficient to significantly increase the star formation activity of cluster galaxies.

Subject headings: Galaxies: individual: (NGC 4435, NGC 4438) – Galaxies: interactions – Ultraviolet: galaxies – Galaxies: clusters: individual: Virgo

1. INTRODUCTION

NGC 4438 (Arp 120) is the clearest example of an ongoing tidal interaction in a nearby cluster of galaxies. Apparently located close to the Virgo cluster center (~ 300 kpc from M87), NGC 4438 is a bulge-dominated late-type spiral showing long tidal tails (30 kpc) thought to be induced by a recent dynamical interaction with the nearby SB0 galaxy NGC 4435. Multifrequency observations covering the electromagnetic spectrum from X-rays (Kotanyi et al. 1983; Machacek et al. 2004) to radio continuum (Hummel & Saikia 1991), including both spectro-photometric and kinematical (Kenney et al. 1995) data, have been carried out in the past to study the nature of this peculiar system. These observations have shown that the violent interaction between the two galaxies per-

turbed the atomic (Cayatte et al. 1990) and molecular (Combes et al. 1988) gas distribution, causing both gas infall toward the center which might have induced nuclear activity (Kenney et al. 1995; Kenney & Yale 2002; Machacek et al. 2004), and gas removal in the external parts displacing part of the gas in the ridge in between the two galaxies (Combes et al. 1988).

Both multifrequency observational data (Kenney et al. 1995; Machacek et al. 2004) and model predictions (Combes et al. 1988; Vollmer et al. 2005) favor a recent (~ 100 Myr) high-velocity, off-center collision between NGC 4435 and NGC 4438.

Except for mild nuclear activity, it is still unclear whether the dynamical interaction between the two galaxies induced extra-nuclear star formation events: the low H α /[NII] ratio and the similar X-ray and H α morphology of NGC 4438 indicate that the H α emission is in this case not due to the ionizing radiation but is probably due to gas cooling phenomena (Machacek et al. 2004).

The UV emission (at ~ 2000 Å) is dominated by young stars of intermediate masses ($2 < M < 5M_{\odot}$, e.g. Boselli et al. 2001) and provides us with an alternative star formation tracer. As part of the Nearby Galaxy Survey (NGS), we have observed the central 12 deg² of the Virgo cluster using the *Galaxy Evolution Explorer* (GALEX). In this paper we present the UV observations of the interacting galaxies NGC 4435 and NGC 4438¹.

2. DATA

The GALEX data used in this work include far-ultraviolet (FUV; $\lambda_{\text{eff}} = 1530\text{Å}$, $\Delta\lambda = 400\text{Å}$) and

¹ A distance of 17 Mpc for Virgo is adopted

¹ Laboratoire d'Astrophysique de Marseille, BP8, Traverse du Siphon, F-13376 Marseille, France

² Observatories of the Carnegie Institution of Washington, 813 Santa Barbara St., Pasadena, CA 91101

³ California Institute of Technology, MC 405-47, 1200 East California Boulevard, Pasadena, CA 91125

⁴ Center for Astrophysical Sciences, The Johns Hopkins University, 3400 N. Charles St., Baltimore, MD 21218

⁵ Center for Space Astrophysics, Yonsei University, Seoul 120-749, Korea

⁶ Department of Physics and Astronomy, The Johns Hopkins University, Homewood Campus, Baltimore, MD 21218

⁷ Space Sciences Laboratory, University of California at Berkeley, 601 Campbell Hall, Berkeley, CA 94720

⁸ NASA/IPAC Extragalactic Database, California Institute of Technology, Mail Code 100-22, 770 S. Wilson Ave., Pasadena, CA 91125

⁹ Laboratory for Astronomy and Solar Physics, NASA Goddard Space Flight Center, Greenbelt, MD 20771

¹⁰ Department of Physics and Astronomy, University of California, Los Angeles, CA 90095

near-ultraviolet (NUV; $\lambda_{\text{eff}} = 2310\text{\AA}$, $\Delta\lambda = 1000\text{\AA}$) images with a circular field of view of radius ~ 0.6 degrees. The spatial resolution is ~ 5 arcsec. Details of the GALEX instrument and data characteristics can be found in Martin et al. (2005) and Morrissey et al. (2005). The data (IR0.2 release) consist of 2 independent GALEX pointings centered at R.A.(J2000)=12h29m01.2s, Dec(J2000)=+13°10'29.6" (819 sec) and R.A.(J2000)=12h25m25.2s, Dec(J2000)=13°10'29.6" (1511 sec), for a total of 2330 sec of integration time.

To study the star formation history of NGC 4438, the UV data have been combined with visible and near-IR images of the galaxy taken from the GOLDmine database (<http://goldmine.mib.infn.it>; Gavazzi et al. 2003), from the SDSS Data release 3 (Abazajian et al. 2004) from the 2MASS survey (Jarrett et al. 2003) and from the CFHT and SUBARU archives. These are $H\alpha+[NII]$ (Boselli & Gavazzi 2002), B (Boselli et al. 2003a), K' (Boselli et al. 1997), u, g, r, i, z SDSS, R CFHT and SUBARU and H 2MASS images. For the main body of the galaxy (region 4 in Fig. 1, see next sect.) we added the integrated spectrum (3500-7000 Å; Gavazzi et al. 2004). The current calibration errors of the NUV and FUV magnitudes are on the order of $\sim 10\%$ (Morrissey et al. 2004), comparable to that at other frequencies.

3. THE UV EMISSION AND THE STAR FORMATION HISTORY OF NGC 4438

Figure 1 shows the UV image of NGC 4438, obtained by combining together the NUV and FUV frames in order to increase the S/N. The UV emission of the galaxy is mostly due to compact, bright regions in the central part of the galaxy (marked as region 4 in Fig. 1), in the northern tidal tail (region 2) and in the section of the southern tail closest to the main body of the galaxy (region 5). The UV emission is mostly diffuse in the extended western part of the northern tail (region 3) and at the edge of the southern tidal tail (region 6). Figure 1 shows the presence of extended and patchy emission to the north-west of the galaxy (~ 15 -25 kpc from the nucleus, marked as region 1). This feature, previously undetected in other visible and/or near-IR bands, is similar to a tidal tail ~ 20 kpc long and ~ 2 kpc wide. A similar smaller region (~ 2 kpc) at ~ 25 kpc from the nucleus is designated region 7. The average NUV surface brightness of these features is ~ 28.5 ABmag arcsec $^{-2}$, while they are undetected in the SUBARU R band (360 sec) image down to a surface brightness limit of ~ 27.8 mag arcsec $^{-2}$.

The RGB image of the galaxy obtained by combining the FUV, NUV and B frames, given in Plate 1, shows the color of the different regions: while the edge of both the northern and the southern tidal tails (region 3 and 6) are red (thus dominated by relatively old stars), regions 2 and 5 as well as the newly discovered regions 1 and 7, have blue colors and seem therefore to be dominated by a younger population. The $H\alpha+[NII]$ emission map, given in Fig. 2 as a contour plot superposed on the NUV image of NGC 4438, shows a lack of massive, ionizing young O-B stars² (Kennicutt 1998) down to a surface

² The $H\alpha+[NII]$ emission observed in region 5 has a different

brightness limit of $\sim 5 \cdot 10^{-17}$ erg s $^{-1}$ cm $^{-2}$ arcsec $^{-2}$. Extraplanar diffuse regions with an excess of UV over $H\alpha$ flux ratio (as that observed at 11 kpc from the disk of M82) are often interpreted as due to the UV radiation produced by the central starburst and locally scattered by diffuse dust (Hoopes et al. 2005). It is unlikely that scattered light is responsible for the UV emission in regions 2 and 5 since it comes from disk HII regions. The steep slope of the UV spectrum ($\beta=-2.32$ and -2.05 , as defined by Kong et al. 2004 respectively for regions 1 and 7) is typical of a recent unreddened starburst (Calzetti 2001) and is unexpected in a scattering scenario since the dust albedo is greater in the NUV than in the FUV (Draine 2003). Furthermore the lack of a powerful central starburst (as in M82) and the large distance of these relatively patchy regions from the nucleus seem to exclude the scattering scenario.

These data suggest that regions 1 and 7 (and to a lesser degree regions 2 and 5) are post starbursts, induced by the violent interaction with NGC 4435, but that they lasted for a relatively short time, since they are not producing young, massive O-B stars any more. This is probably because the atomic and molecular gases, needed to feed star formation, have been removed during the interaction (Combes et al. 1988; Vollmer et al. 2005)

In order to age-date the starburst and reconstruct the star formation history of the galaxy, we have determined the spectral energy distribution (SED) of these seven regions (see Plate 1) and then fitted them with a model of galaxy evolution. To this end we make the assumption that dust attenuating the SED is present only in region 4, where we correct the UV to near-IR data using the far-IR to UV flux ratio as done in Boselli et al. (2003a). This restricted application is reasonable since no dust emission has been observed in the tidal tails with ISOCAM (Boselli et al. 2003b); furthermore, in regions 1 and 7, dust is unexpected since it has not yet been produced by the young stellar population, as confirmed by the steep β parameter.

We assume that NGC 4438 was a normal, late-type object before interacting with NGC 4435. The models of chemo-spectrophotometric evolution of normal, spiral galaxies of Boissier & Prantzos (2000), updated with an empirically-determined star formation law (Boissier et al. 2003) are used to reconstruct the SED of the galaxy stellar population before the interaction. The two parameters of the model (spin λ and rotational velocity V_C) are constrained by the total H-band luminosity, the velocity rotation and by the SED of the main body of the galaxy (region 4), composed by an old population with no significant contribution from the recent starburst (leading to $\lambda=0.01$ and $V_C=290$ km s $^{-1}$). We then assume that the underlying stellar population of each region, if present, is the one given by the model and removed from the main body of the galaxy by the tidal interaction, while the younger population is produced by the induced star-

morphology than the UV one: this evidence confirms the conclusions of Machacek et al. (2004) that the $H\alpha+[NII]$ emission is not due to the ionizing radiation but is probably associated to the cooling gas

³ The upper limit of the HI surface density for these regions is $\sim 1 M_{\odot}$ pc $^{-2}$ (Cayatte et al. 1990)

burst. For each region, we combine the evolved stellar population with an instantaneous burst of star formation obtained using Starburst 99 (Leitherer et al. 1999) for a solar metallicity and a Salpeter IMF between 1 and 100 M_{\odot} . For each age and intensity of the burst, we determine the best combination of evolved population+ burst by fitting the FUV to K band SED and rejecting solutions in disagreement with the upper limits. We then adopt the age corresponding to the lowest reduced χ^2 ⁴. This exercise gives a consistent result: the strong UV emission of regions 1 and 7 is due to a coeval starburst \sim 6-20 Myr old (see Panel 1). The age and the duration of the starburst are strongly constrained both by the lack of H α emission and by the blue UV slope of the spectrum (lower limit to the age) and by the lack of an old stellar population (upper limit to the duration). Regions 2 and 5 are well fitted by an older starburst (\geq 100 Myr) which ended \sim 10 Myr ago as indicated by the lack of any H α emission and a redder UV slope ($\beta=-0.33$ and -0.67 in regions 2 and 5 respectively). While the fraction of stars produced by this burst is dominant in regions 1 and 7, the sum of the stars produced by the burst in all regions (including the inner part) contributes to the total galaxy stellar mass by less than 0.1 %, an extremely low value for such a violent interaction.

4. DISCUSSION AND CONCLUSION

These observations have major consequences in constraining the evolution of cluster galaxies. A high-velocity off-center collision between two galaxies of relatively similar mass, whose violence is able to perturb the stellar distribution producing important tidal tails, is insufficient to induce a significant instantaneous starburst. This result might be representative only of the nearby Universe where encounters of gas-rich galaxies are probably rare since clusters are dominated by gas-poor early-type galaxies such as the companion galaxy NGC 4435. It is conceivable, however, that at higher redshifts, where clusters are forming, stellar masses produced by a starburst induced by interactions predicted by the models of Moore et al. (1996; galaxy

⁴ All ages with $\chi^2 < 1$ are acceptable solutions. Given the small number of photometric points available for regions 1 and 7 (2 GALEX bands), the fitted solution for a combination of a burst and an old population (two parameters) can be almost perfect (resulting in very low χ^2 , $\leq 10^{-2}$), as long as the obtained fit is in

harassment) might be more important given the higher fraction of gas-rich galaxies.

The other interesting result is the long time differential between the age of the interaction (\sim 100 Myr as determined by dynamical simulations, Combes et al. 1988; Vollmer et al. 2005) and the beginning of the starburst (\sim 10 Myr in regions 1 and 7, \sim 100 Myr in regions 2 and 5). This result is totally consistent with the models of Mihos et al. (1991) that predict for close-by encounters an enhancement of the star formation activity in the inner disk during some 100 Myr, stopping once the gas reservoir is exhausted as in NGC 4438. In the tidal tails, on the contrary, star formation is expected to increase after \sim 100 Myr, the time needed by the gas to re-collapse, but then ceasing after a few Myr because the expansion of the tidal tail brings the gas surface density to subcritical values (no HI and CO has been detected in these regions). If these systems are dynamically stable and survive the interaction, they might be at the origin of some dwarf galaxies in the cluster similar to those observed in the Stephan's Quintet by Mendes de Oliveira et al. (2004) or in other interacting systems (Neff et al. 2005; Hibbard et al. 2005, Saviane et al. 2004) Being produced by a single starburst, these gas poor systems might evolve into dwarf ellipticals, typical of rich clusters. Otherwise they will simply increase the fraction of unbound stars, contributing to the Virgo intracluster light (Willman et al. 2004).

GALEX (Galaxy Evolution Explorer) is a NASA Small Explorer, launched in April 2003. We gratefully acknowledge NASA's support for construction, operation, and science analysis for the GALEX mission, developed in cooperation with the Centre National d'Etudes Spatiales of France and the Korean Ministry of Science and Technology. We wish to thank the referee, V. Charmandaris, for precious comments which helped improving the quality of the manuscript.

agreement with the limits at other wavelengths. Whenever the fit produces a SED not satisfying a detection limit, this solution is rejected.

REFERENCES

- Abazajian, K., et al., 2004, astro-ph/0410239
 Boissier, S. & Prantzos, N., 2000, MNRAS, 312, 398
 Boissier, S., Prantzos, N., Boselli, A. & Gavazzi, G., 2003, MNRAS, 346, 1215
 Boselli, A. & Gavazzi, G., 2002, A&A, 386, 124
 Boselli, A., Tuffs, R., Gavazzi, G., Hippelein, H. & Pierini, D., 1997, A&AS, 121, 507
 Boselli, A., Gavazzi, G., Donas, J. & Scodreggio, M., 2001, AJ, 121, 753
 Boselli, A., Gavazzi, G. & Sanvito, G., 2003a, A&A, 402, 37
 Boselli, A., Sauvage, M., Lequeux, J., Donati, A. & Gavazzi, G., 2003b, A&A, 406, 867
 Calzetti, D., 2001, PASP, 113, 1449
 Cayatte, V., van Gorkom, J., Balkowski, C., & Kotanyi, C., 1990, AJ, 100, 604
 Combes, F., Dupraz, C., Casoli, F. & Pagani, L., 1988, A&A, 203, L9
 Draine, B.T., 2003, ApJ, 598, 1017
 Gavazzi, G., Boselli, A., Donati, A., Franzetti, P. & Scodreggio, M., 2003, A&A, 400, 451
 Gavazzi, G., Zaccardo, A., Sanvito, G., Boselli, A. & Bonfanti, C., 2004, A&A, 417, 499
 Jarrett, T., Chester, T., Cutri, R., Schneider, S. & Huchra, J., 2003, AJ, 125, 525
 Hibbard, J., et al., 2005, ApJL, Galex special issue (astro-ph/0411352)
 Hoopes, C., et al., 2005, ApJL, Galex special issue (astro-ph/0411309)
 Hummel, E. & Saikia, D., 1991, A&A, 249, 43
 Keel, W. & Wehrle, A., 1993, AJ, 106, 236
 Kenney, J. & Yale, E., 2002, ApJ, 567, 865
 Kenney, J., Rubin, V., Planesas, P. & Young, J., 1995, ApJ, 438, 135
 Kennicutt, R., 1998, ARA&A, 36, 189
 Kong, X., Charlot, S., Brinchmann, J. & Fall, S., 2004, MNRAS, 349, 769
 Kotanyi, C., van Gorkom, J. & Ekers, R., 1983, ApJ, 273, L7
 Leitherer, C., et al., 1999, ApJS, 123, 3
 Machacek, M., Jones, C. & Forman, W., 2004, ApJ, 610, 183

- Martin, C., et al., 2005, ApJL, GaleX special issue (astro-ph/0411302)
- Mendes de Oliveira, C., Cypriano, E., Sodr e, L., Balkowski, C., 2004, ApJ, 605, L20
- Mihos, C., Richstone, D., Bothun, G., 1991, ApJ, 377, 72
- Moore, B., Katz, N., Lake, G., Dressler, A. & Oemler, A., 1996, Nat, 379, 613
- Morrissey, P., et al., 2005, ApJL, GaleX special issue (astro-ph/0411310)
- Neff, S., et al., 2005, ApJL, GaleX special issue (astro-ph/0411372)
- Saviane, I., Hibbard, J., Rich, M., 2004, AJ, 127, 660
- Vollmer, B., Braine, J., Combes, F. & Sofue, Y., 2005, submitted to A&A
- Willman, B., Governato, F., Wadsley, J. & Quinn, 2004, MNRAS, 355, 159

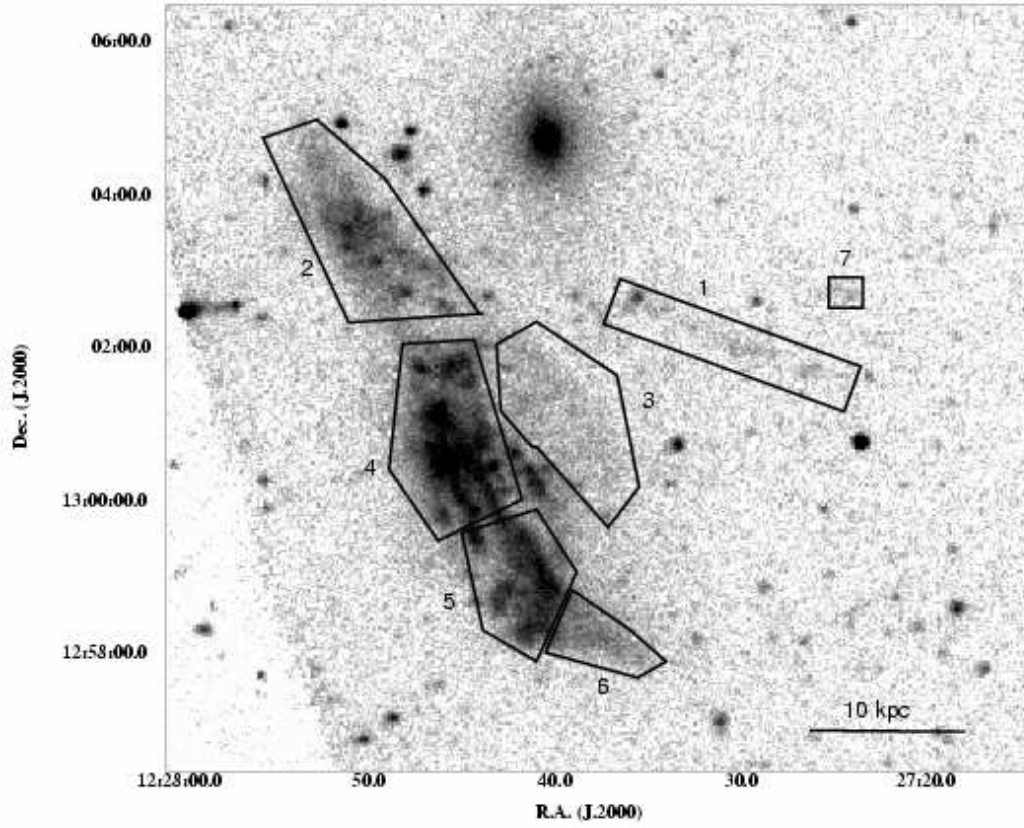


FIG. 1.— The combined NUV and FUV image of NGC 4438. The regions described in sect. 3 of the text are labeled 1 to 7. The horizontal line is 10 kpc long (assuming a distance of 17 Mpc).

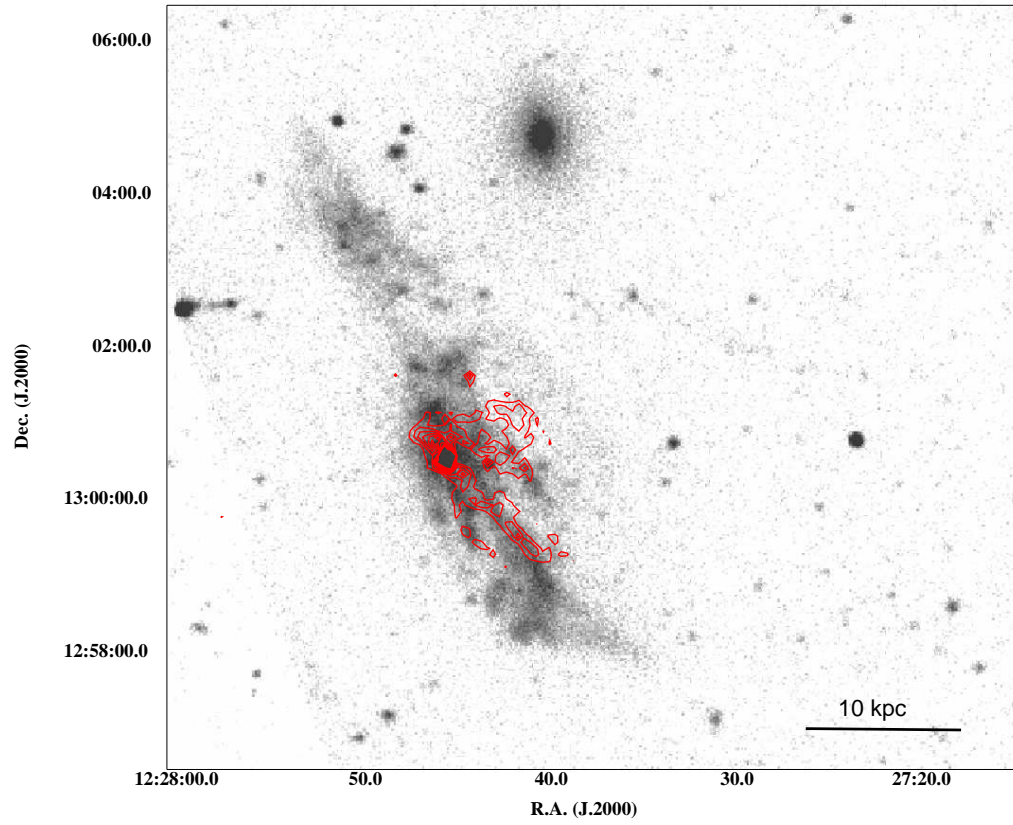


FIG. 2.— The $H\alpha+[NII]$ contours (red, in arbitrary scale, in between $8 \cdot 10^{-17}$ and $6 \cdot 10^{-16} \text{ erg cm}^{-2} \text{ s}^{-2} \text{ arcsec}^{-2}$, with $\sigma = 5 \cdot 10^{-17} \text{ erg cm}^{-2} \text{ s}^{-2} \text{ arcsec}^{-2}$, from Boselli & Gavazzi (2002)) are superposed to the NUV gray-level image of NGC 4438.

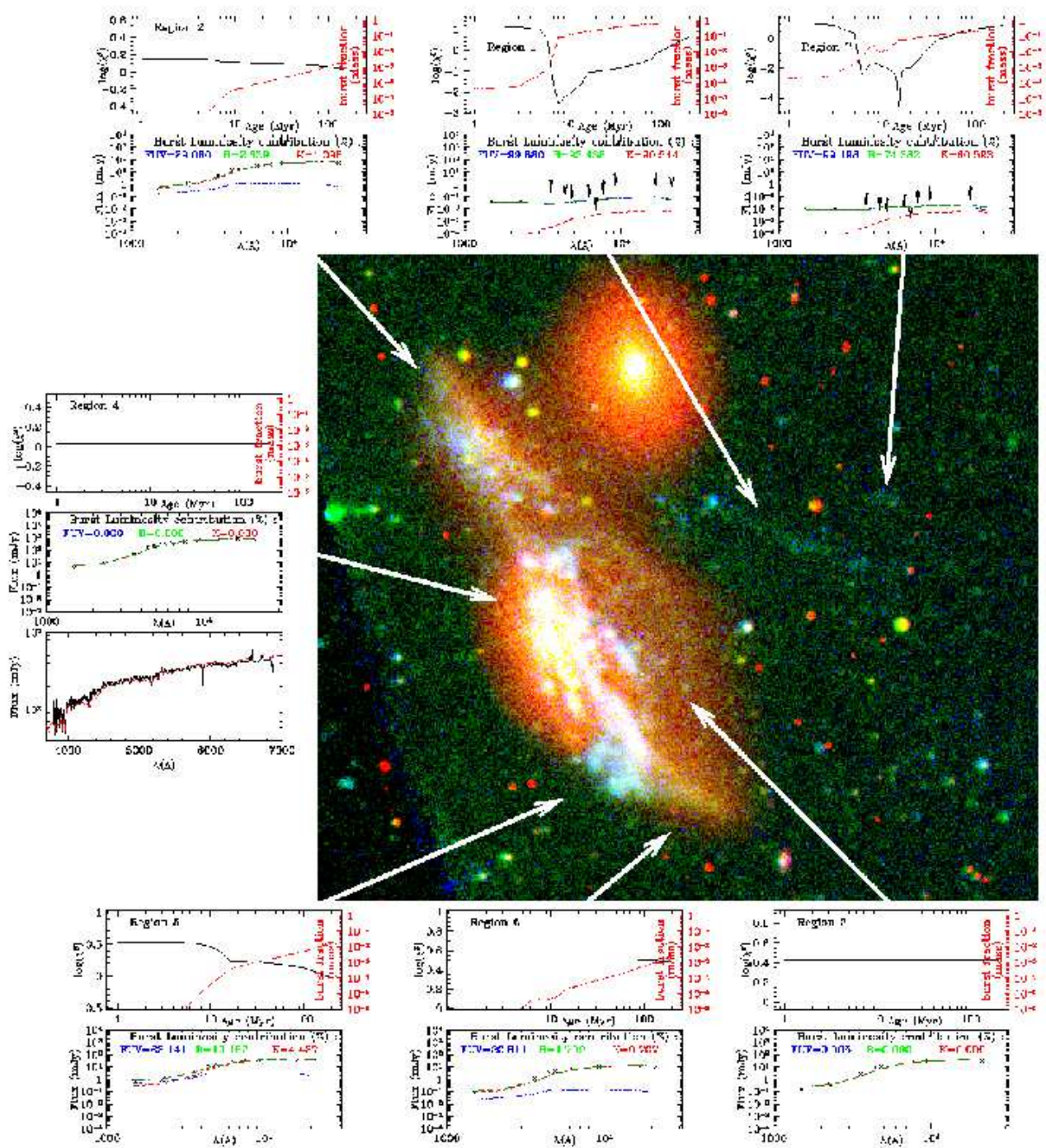


FIG. 3.— The RGB (FUV=blue, NUV=green, B=red) color map of NGC 4438 and NGC 4435. The SED of each region defined in Fig. 1 are given in the lower plot of each frame. Crosses indicate the observed data, arrows upper limits (in mJy), the red dashed line the evolved population fit as determined by the model of Boissier & Prantzos (2000), the dotted blue line the starburst SED (from Starburst 99) and the dashed green line the combined fitting model. The burst luminosity contribution (for the age corresponding to the minimum χ^2) in the band FUV, B and K is also given. The upper panel gives the variation of the reduced χ^2 parameter (black continuum line, in logarithmic scale) and of the burst mass fraction (red dotted line) as a function of the age of the burst (in Myr). The lower panel of region 4 gives the integrated 3500 to 7000 Å, $R=1000$ spectrum of the main body of the galaxy (black continuum line) compared to the fitted model (red dashed line).